Performance of a single $Pb_{1-x}Sn_xTe(In)$ terahertz photodetector

Dmitry Khokhlov

Physics Department
M.V. Lomonosov Moscow State University

M. V. Lomonosov Moscow State University
FACULTY OF PHYSICS

Cooperation

- M.V. Lomonosov Moscow State University
  - Ludmila Ryabova
  - Dmitry Dolzhenko
  - Vladimir Chernichkin
- Institute of Applied Physics, Kishinev, Moldova
  - Andrey Nicorici
- University of Beer Sheva, Israel
  - Vladimir Kasiyan
  - Zinovy Dashevsky
- University of Regensburg
  - Sergey Ganichev
  - Sergey Danilov
- A.F. Ioffe Physical-Technical Institute, St-Petersburg
  - Vassily Bel'kov

Russian Space Missions in Terahertz and Millimeter Ranges

- RADIOASTRON
  - Test launch – 21 January 2011
  - Launch scheduled for May 2011
- MILLIMETRON
  - Launch scheduled for 2017-2018
  - The project is accepted by the Russian Space Agency
  - Supported by the German Space Agency
  - Pending support from the European Space Agency

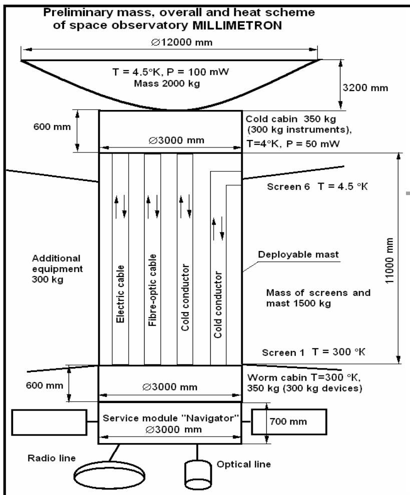

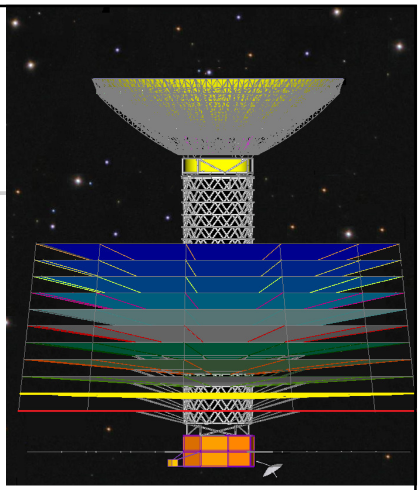

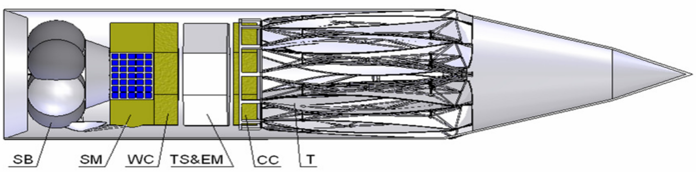

Proton-M launcher, L2 orbit, 4500+2100 kg.

SB – space buster DM, SM – service module, WC – warm cabin, TS&EM – thermal screens & expanding mast, CC – cold cabin, T – telescope.

The Space Observatory in the single-dish mode

Telescope:
Primary mirror diameter 12 m, surface RMS accuracy 10 μm, diffraction beam 4'' and field of view 4.5' at 1.5 THz.

Bolometer arrays:
wavelength ranges 0.2-0.4 mm, and 0.7-1.4 mm
HPBW beam (at 1.5 THz) 4''

Low resolution spectropolarimeter:
wavelength range 0.02-0.8 mm
spectral resolution R = 3

Medium resolution spectrometers:
wavelength ranges 0.03-0.1 mm, and 0.1-0.8 mm
spectral resolution R = 1000

High resolution spectrometer:
wavelength ranges 0.05 – 0.3 mm
spectral resolution $R = 10^6$

Bolometric sensitivity: at 1 THz, NEP = 10^{-19} $W(s)^{0.5}$, A = 100 m^2, R=3 and 1 h integration $5 \cdot 10^{-9}$ Jy (1 σ)

Undoped Lead Telluride-Based Alloys

PbTe: narrow-gap semiconductor:

- 1. Cubic face-centered lattice of the NaCl type
- 2. Direct gap E_g = 190 meV at T = 0 K at the L-point of the Brillouin zone
- 3. High dielectric constant $\varepsilon \sim 10^3$.
- 4. Small effective masses $m \sim 10^{-2}\ m_e$.

$Pb_{1-x}Sn_xTe$ Solid Solutions:

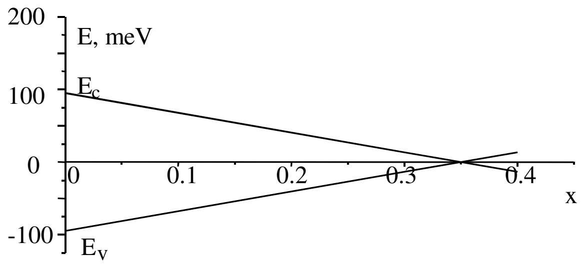

Origin of free carriers:
deviation from stoikhiometry ~ 10^{-3}.
As-grown alloys: $n,p \sim 10^{18}$-10^{19} cm^{-3}
Long-term annealing: $n,p > 10^{16}$ cm^{-3}

Effects Appearing upon Doping

Fermi Level Pinning Effect.

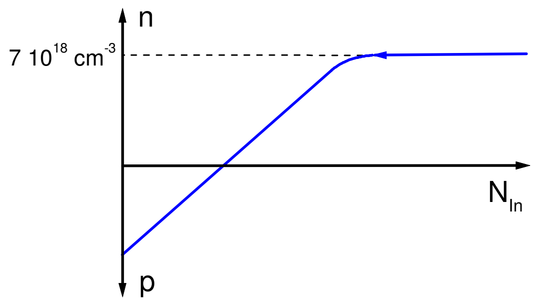

PbTe(In), $N_{In} > N_i$

Consequences

- 1. **Absolute reproducibility** of the sample parameters independently of the growth technique. Therefore **low production costs**.
- 2. Extremely **high spatial homogeneity**.
- 3. **High radiation hardness** (stable to hard radiation fluxes up to 10^{17} cm^{-2})

Fermi Level Pinning in the $Pb_{1-x}Sn_xTe(In)$ Alloys.

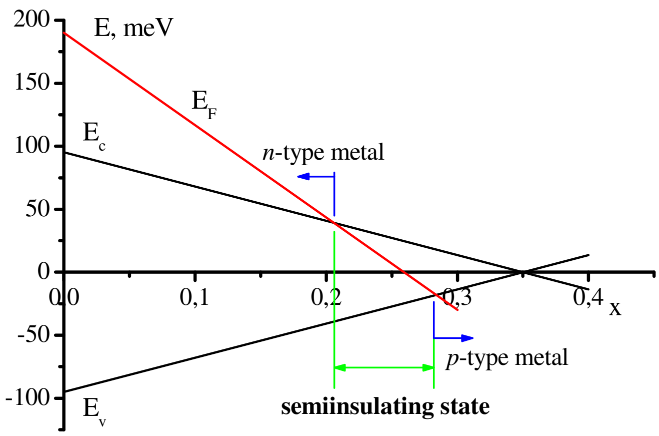

Persistent Photoconductivity

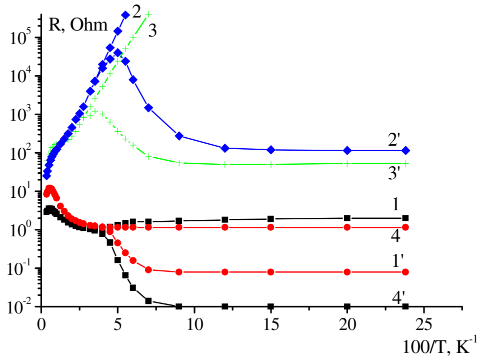

Temperature dependence of the sample resistance *R* measured in darkness (1-4) and under infrared illumination (1'-4') in alloys with *x* = 0.22 (1, 1'), 0.26 (2, 2'), 0.27 (3, 3') and 0.29 (4, 4')

Photoconductivity Kinetics

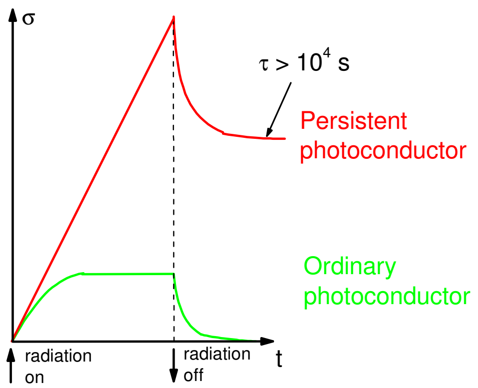

Long lifetime of the photoexcited electrons is due to a barrier between local and extended electron states – **DX-like impurity centers.**

Shubnikov – de Haas oscillations induced by illumination

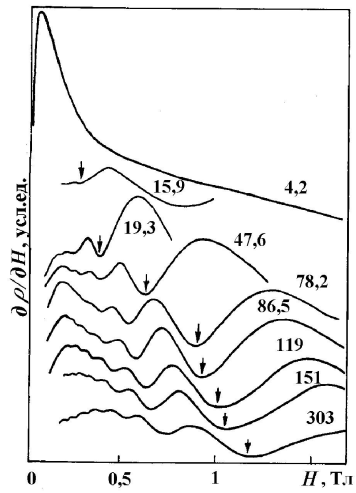

Mixed valence model: picture

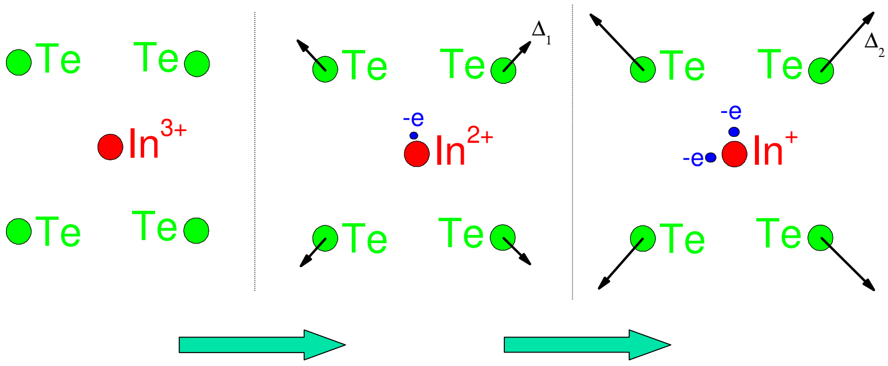

Model for long-term relaxation processes

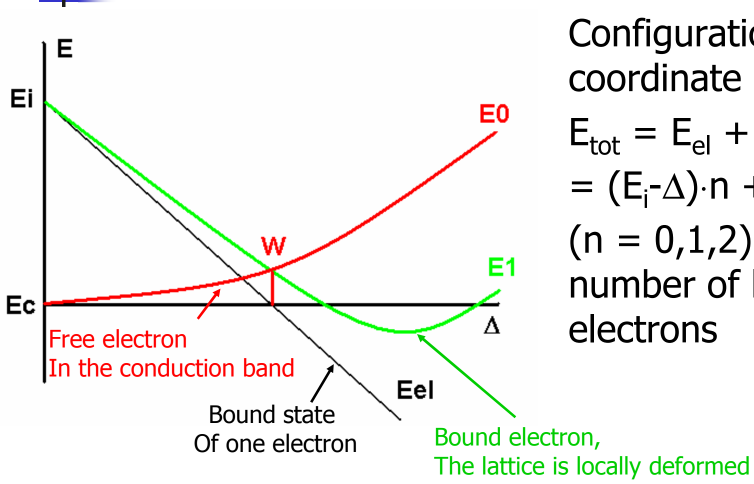

Configuration-coordinate diagram

$E_{tot} = E_{el} + E_{lat} =$

$= (E_i - \Delta)\cdot n + \Delta^2/2\Delta_0$

$(n = 0,1,2)$ – number of localized electrons

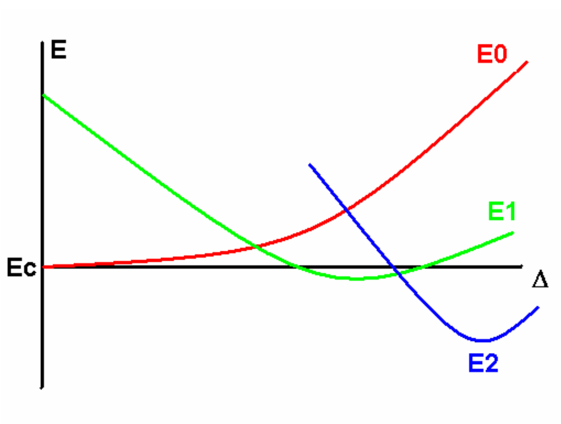

- E_2 – ground local state;
- E_1 – metastable local state

Photoconductivity kinetics

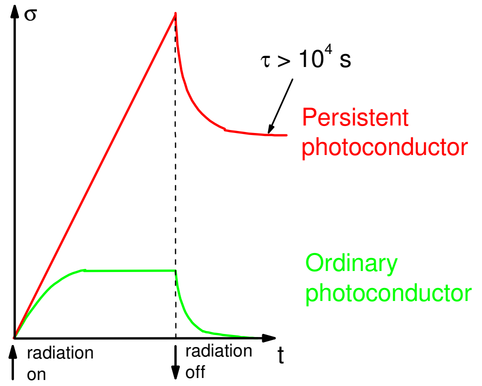

Fast relaxation is due to transitions to the metastable state, slow relaxation corresponds to transitions to the ground local state

Local metastable states

The metastable states are responsible for appearance of a range of strong effects:

- Enhanced diamagnetic response up to 1% of ideal
- Enhancement of effectic dielectric permittivity up to 10^5 at TeraHertz illumination
- Giant negative magnetoresistance up to 10^6
- Persistent photoconductivity in the terahertz spectral range

Spectral response

- Two approaches
  - Low-background: sample screened from the background radiation, low-intensity sources
  - High-background: sample is not screened from the background radiation, high-intensity sources

High-background approach

- Laser wavelengths:
  90, 148, 280, 496 μm
- Pulse length: 100 ns
- Power in a pulse: up to 30 kW
- Sample temperature: 4.2 – 300 K
- Samples: single crystalline $Pb_{0.75}Sn_{0.25}Te(In)$, polycrystalline PbTe(In) films

Fermi Level Pinning in the $Pb_{1-x}Sn_xTe(In)$ Alloys.

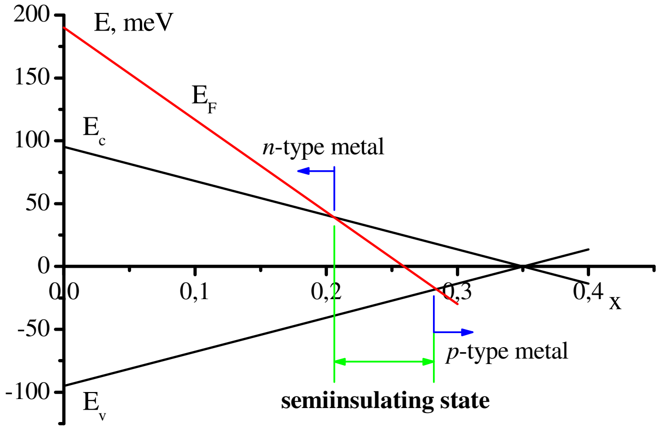

Photoconductivity kinetics

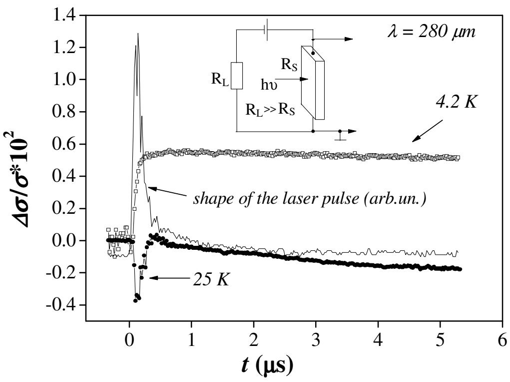

Time profile of a laser pulse and photoconductivity kinetics
at different temperatures

Photoconductivity mechanisms

- Negative photoconductivity: electron gas heating, change in electron mobility
- Positive photoconductivity: generation of non-equilibrium electrons from metastable impurity states, change in free electron concentration

Dependence of the photoresponse amplitude on the radiation wavelength

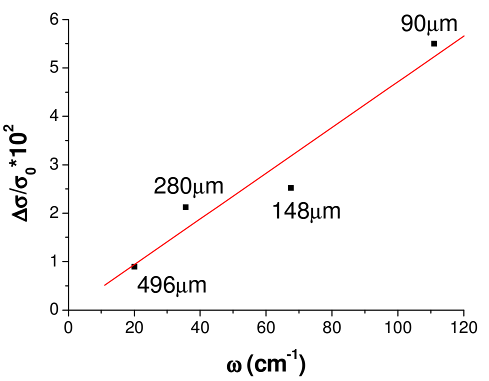

N_{qu}=8.7 10^{-24} s^{-1}

Considerable photoresponse is observed up the wavelength of 496 µm which is **more than two times higher** than the previous record value of 220 µm observed for uniaxially stressed Ge(Ga)

Linear extrapolation of the quantum efficiency to the zero photoresponse gives the cut-off energy E_{red}=0!

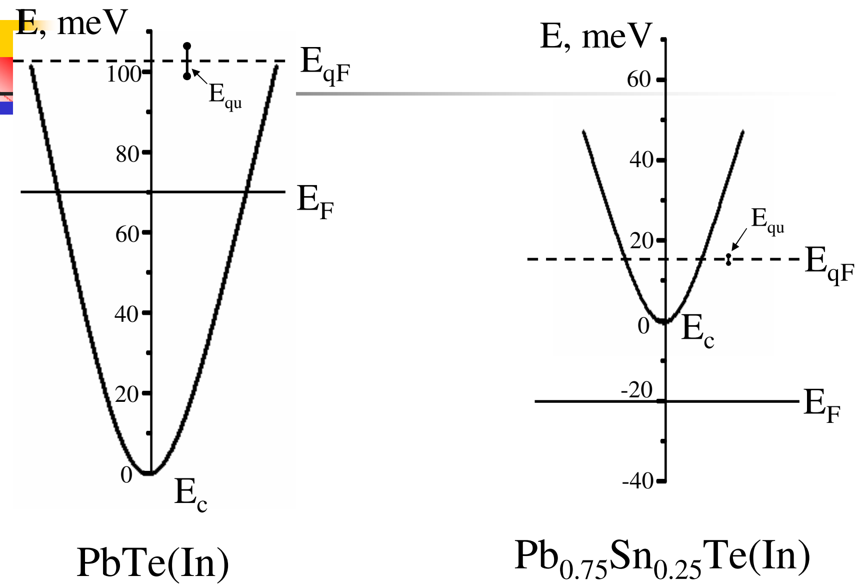

New type of local states in semiconductors

A new type of semiconductor local states which are linked not to a definite position in the energy spectrum, but to the quasiFermi level position which may be tuned by photoexcitation.

Low-background approach

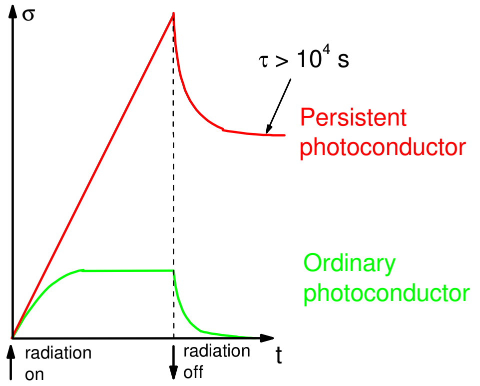

Integration increases the signal-to noise ratio

but

It is important to be able to quench fast the persistent photoconductivity

Quenching of the Persistent Photoconductivity

- 1. **Thermal quenching:** heating to 25 K and cooling down: too slow process.
- 2. **Microwave quenching:** application of microwave pulses to the samples

  $f = 250$ MHz, $P = 0.9$ W, $\Delta t = 10$ μs

Operation of an "integrating" photodetector

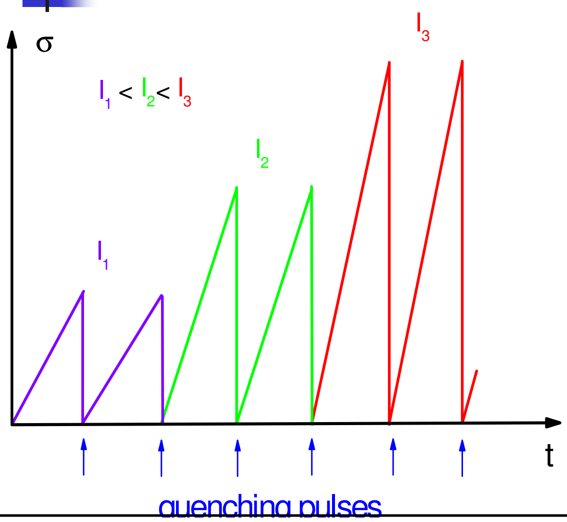

Options:
1. Internal modulation
2. External modulation

Usual set up

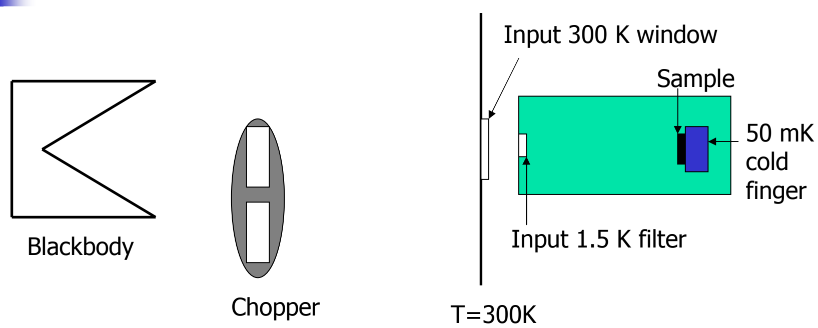

Background power $1.4 * 10^{-13}$ W
Fluctuations $7.3 * 10^{-18}$ W/Hz$^{1/2}$

Cell construction

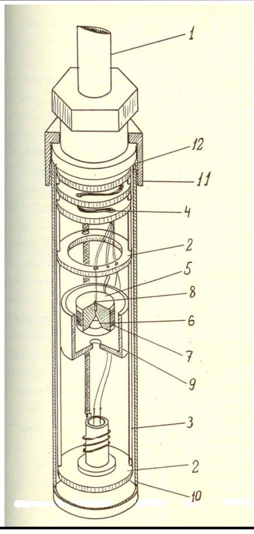

Key elements

- 2 – sample holder
- 5 – heater
- 6 – blackbody opening
- 7 – blackbody
- 8 – thermocouple
- 9 – thermal screen
- 10 – copper cell

Electrical connections

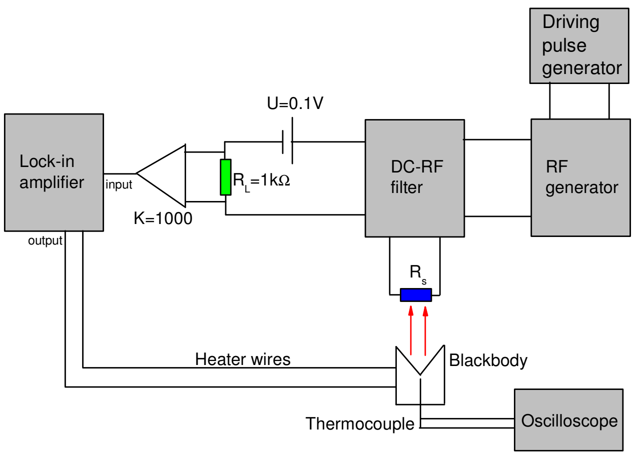

Blackbody temperature modulation

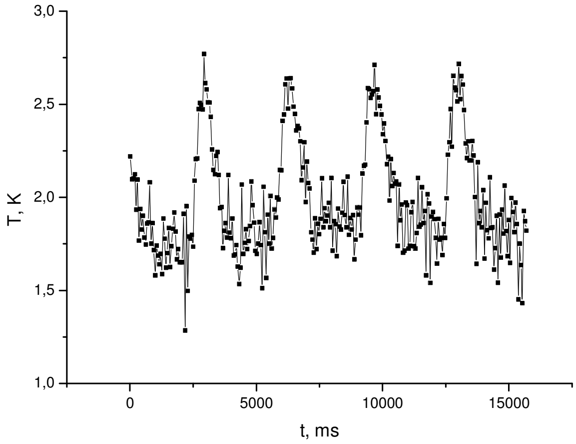

Performance at 1.57 K

Single photodetector operating in the regime of the periodical accumulation and successive fast quenching of the photosignal.

- operating temperature 1.57 K;
- wavelenghth 350 μm (defined by the filter, Q=4);
- area 300*200 μm;
- quenching rate 1000 Hz;
- blackbody modulation rate 0.3 Hz;
- lock-in amplifier integration time 100 s;
- Blackbody temperature providing S/N=1 T_{bb}=2.7 K
- NEP ~ **6×10^{-20}** W/$Hz^{1/2}$ **!!!**

Directions of the future activities

- Measurements of the photon noise
- Single photon counting? Why not
- Development of the portable readout electronics
- Development of linear arrays and full-scale arrays
- Development of tunable terahertz filters
- Development of a system for passive terahertz vision in medical applications
- Investigation for possibilities of application in space missions

Summary

- We have observed a new type of semiconductor local states which are linked not to a definite position in the energy spectrum, but to the quasiFermi level position
- We have demonstrated a record low NEP = $\mathbf{6\times10^{-20}}$ W/Hz$^{1/2}$ for a single photodetector operating in the regime of the periodical accumulation and successive fast quenching of the photosignal, with the operating temperature 1.57 K at the wavelength of 350 μm